

Supporting information

Dynamics of oligomer and amyloid fibril formation by yeast prion Sup35 observed by high-speed atomic force microscopy

Hiroki Konno, Takahiro Watanabe-Nakayama, Takayuki Uchihashi, Momoko Okuda, Liwen Zhu, Noriyuki Kodera, Yousuke Kikuchi, Toshio Ando and Hideki Taguchi

Fig. S1. HS-AFM imaging of Sup35NM oligomers at different concentrations from 0.5 μM .

(A) Height distributions of the diluted oligomers to a lower concentration. 8 M urea-denatured Sup35NM (50 μM) was diluted to 0.5 μM with Buffer A containing 5 mM potassium phosphate (pH 7.3), 150 mM NaCl, 25 mM KCl, and 1 mM dithiothreitol, followed by an incubation at room temperature for 3 h in solution. After confirmation of oligomer formation, the solution of oligomers was diluted to 10 nM and incubated at room temperature for 3 h in solution before height measurement with HS-AFM. The corresponding solid line is most probable Gaussian fitting obtained with 3.96 ± 1.14 nm for mean height \pm S.D. (B) Time course of height distribution of Sup35NM oligomers observed when Sup35NM was diluted to 10 nM. (C) Representative height histograms of oligomers formed when 10 nM Sup35NM was incubated for 60 (*blue*) and 120 (*red*) min (highlighted by dashed *blue* and *red* lines in B). (D) Time course of height distribution of Sup35NM oligomers observed when Sup35NM was incubated at 1.5 μM .

Fig. S2. Effect of surface property of substrate for Sup35NM oligomer and fibril formation.

0.5 μM of Sup35NM monomers were incubated at room temperature (25 $^{\circ}\text{C}$) for 3h on a silane-coated mica (APTES-mica), which has an opposite electrostatic property compared to conventional bare mica surface. Bar, 500 nm. Z-scale, 20 nm. Imaging rate, 0.2 fps. The white arrows indicate higher particles than the 3~4 nm oligomer, which were observed on the APTES-mica even before adding of the Sup35NM monomer. *Inset*, the magnified HS-AFM image. Bar, 20 nm. Z-scale, 6 nm. Imaging rate, 5 fps.

Fig. S3. Fibril growth speed during different incubation periods.

(A) Time courses of length change of Sup35NM fibrils during different incubation periods of 0–30 min (*left*), 30–60 min (*center*), and 60–90 min (*right*) after the addition of fresh monomers to

performed fibrils. (B) Distributions of fibril growth speed observed during the indicated elapsed times after the addition of monomeric Sup35NM.

Fig. S4. Effect of ionic strength on the neighboring distances between particles and between fibril and particles.

Bar graphs showing inter-particle (*open boxes*) and fibril-particle (*closed boxes*) distances observed in the presence of 50, 150, 500, and 1,000 mM NaCl. The mean distance in each experimental condition was compared with the distance in the other conditions: * $p < 0.05$; ** $p < 0.01$; *** $p < 0.001$; note that significant differences were observed between the inter-particle and the fibril-particle distances except in 500 mM NaCl, and that the inter-particle distance in 50 mM NaCl was also significantly different from those in the other salt conditions. The P value of the t test for the inter-particle seems to be low despite the large error bar since the sample number of the distance of inter-particle is 1,700-2,000 for each condition of salt concentration. The sample numbers are 1,983 in 50 mM NaCl, 1,786 in 150 mM NaCl, 1,956 in 500 mM NaCl, 1,891 in 1,000 mM NaCl, respectively. The sample numbers of the distance of the fibril-particle are 20 in 50 mM NaCl, 23 in 150 mM NaCl, 20 in 500 mM NaCl, 21 in 1,000 mM NaCl, respectively.

Fig. S5. HS-AFM imaging of the end and the lateral side regions of a Sup35NM fibril at high temporal resolution.

(A) Representative HS-AFM images showing interaction between Sup35NM fibril end and oligomers. Z-scale, 10 nm. Bar, 10 nm. Imaging rate, 16.7 fps. The white arrows and the dashed white arrow represent oligomers and the fibril end, respectively. (B) Two representative HS-AFM images of the lateral side of fibrils. Z-scale, 10 nm. Bar, 10 nm. Imaging rate, 16.7 fps. The white arrows and the dashed white arrow represent oligomers and a fibril, respectively.

Fig. S6. The protein disorder prediction for Sup35NM.

Disordered regions in Sup35NM were predicted using PONDR VL-XT.

Movie S1. HS-AFM movie showing Sup35NM fibril growth.

Z-scale, 10 nm. Scan size, $1,000 \times 1,000 \text{ nm}^2$. Imaging rate, 0.1 fps. The movie is played back at $\times 90$ higher speed. Total recording time, 31min.

Movie S2. HS-AFM movie showing fluctuations of unstructured regions from a Sup35NM oligomer.

HS-AFM images were captured for Sup35 oligomerization after the initiation of the aggregation reaction. Z-scale, 5 nm. Scan size, $200 \times 200 \text{ nm}^2$. Imaging rate, 16.7 fps. The movie is played back at $\times 6$ higher speed. Total recording time, 20 sec.

Movie S3. HS-AFM movie showing a Sup35NM fibril end.

HS-AFM images were captured for an end region of a Sup35NM fibril in the presence of Sup35NM oligomers. Z-scale, 10 nm. Scan size, $50 \times 50 \text{ nm}^2$. Imaging rate, 16.7 fps.

Movie 4. HS-AFM movie showing a lateral side of the Sup35NM fibril.

HS-AFM images were captured for a lateral side of a Sup35NM fibril in the presence of Sup35NM oligomers. Z-scale, 10 nm. Scan size, $50 \times 50 \text{ nm}^2$. Imaging rate, 16.7 fps.

Fig. S1

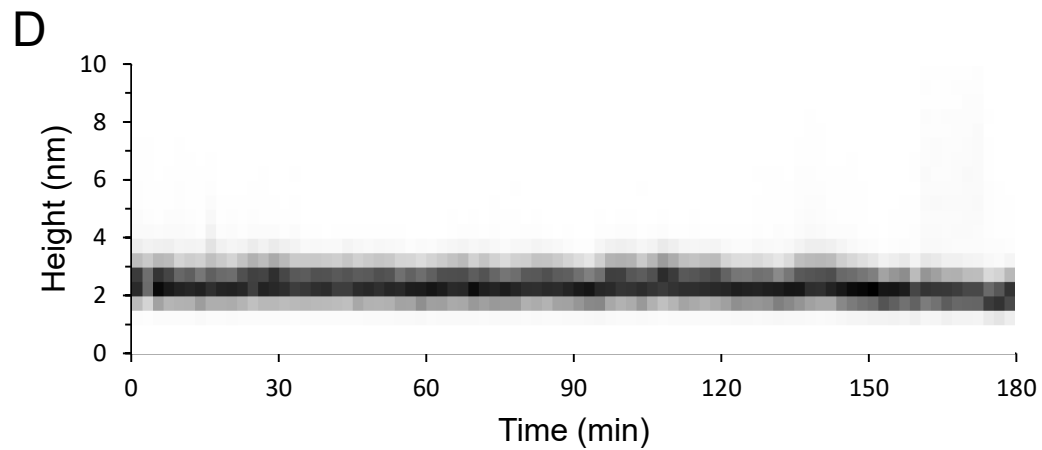
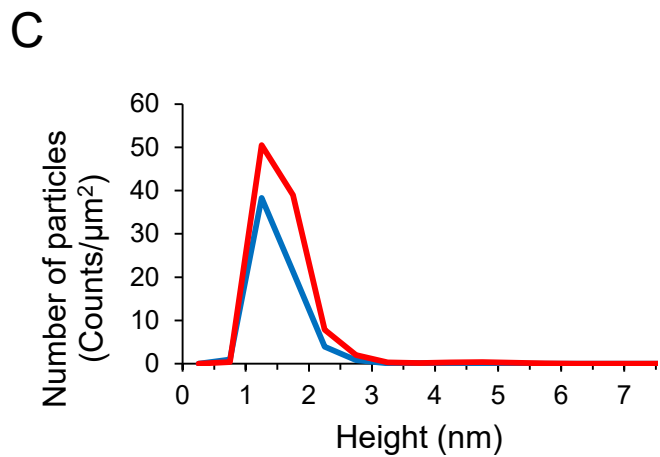
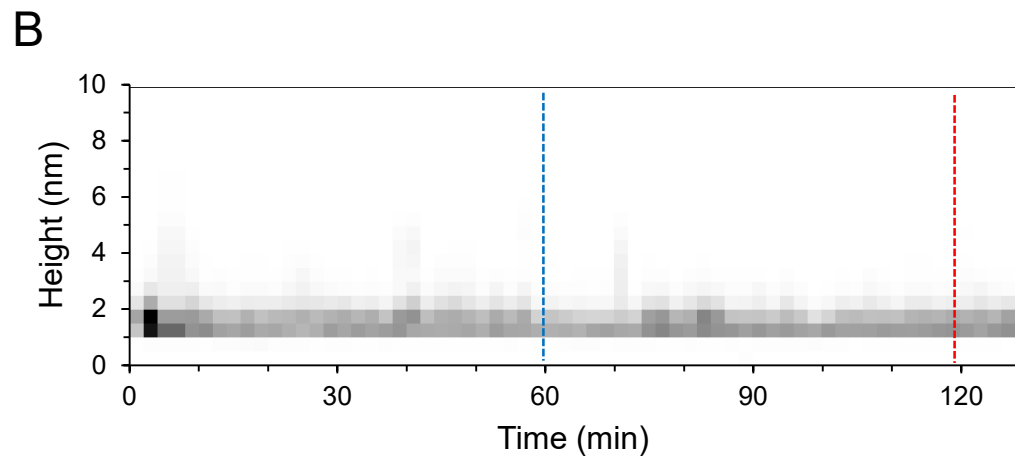
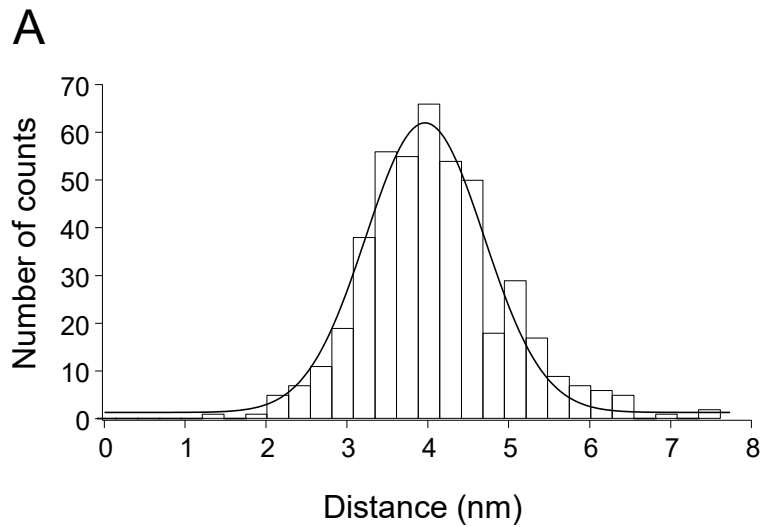


Fig. S2

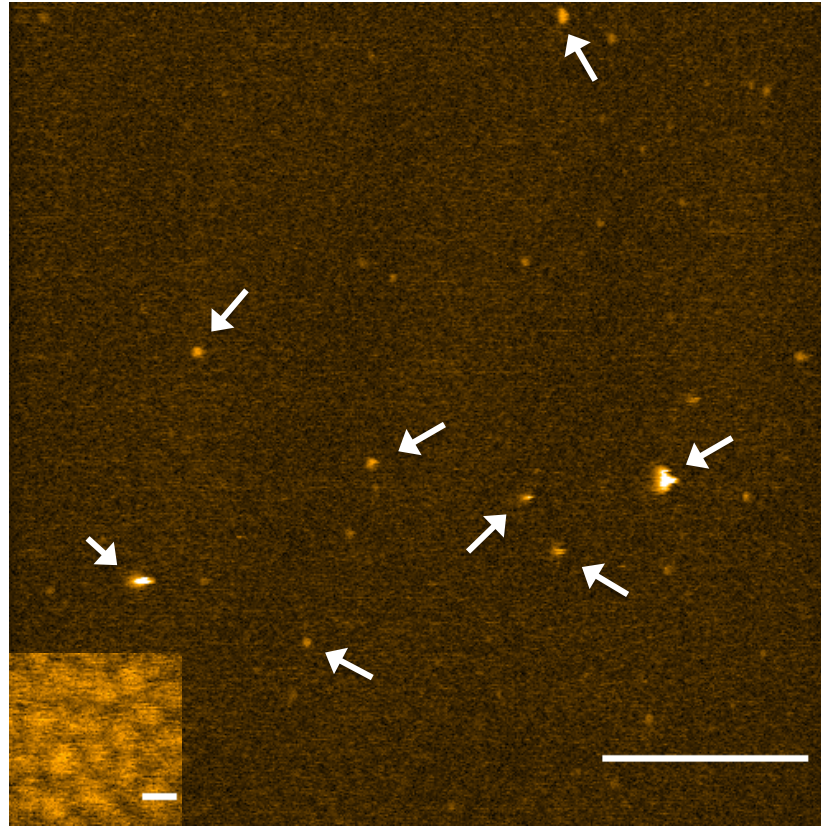


Fig. S3

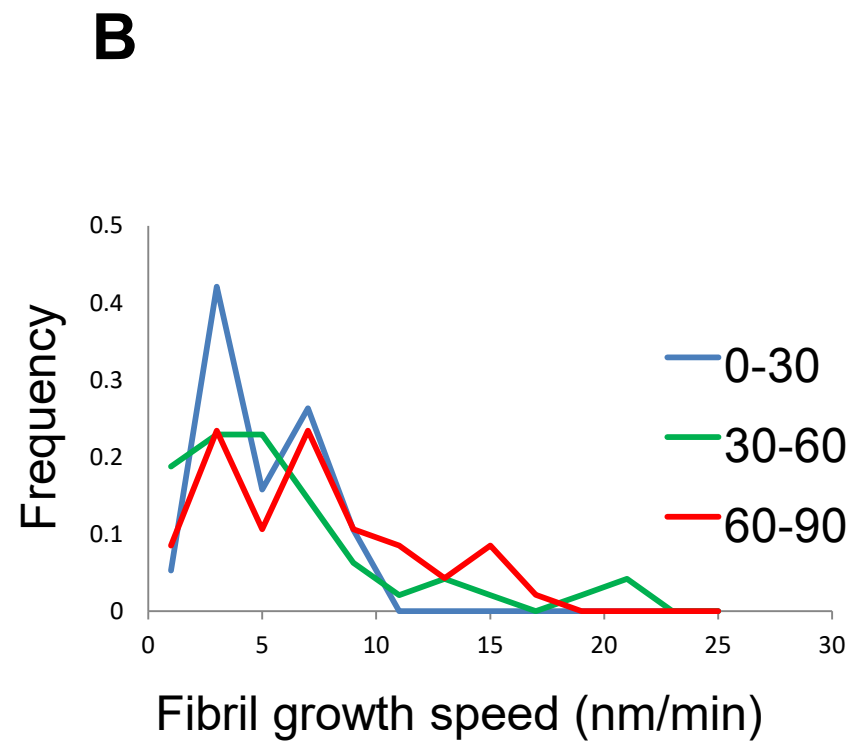
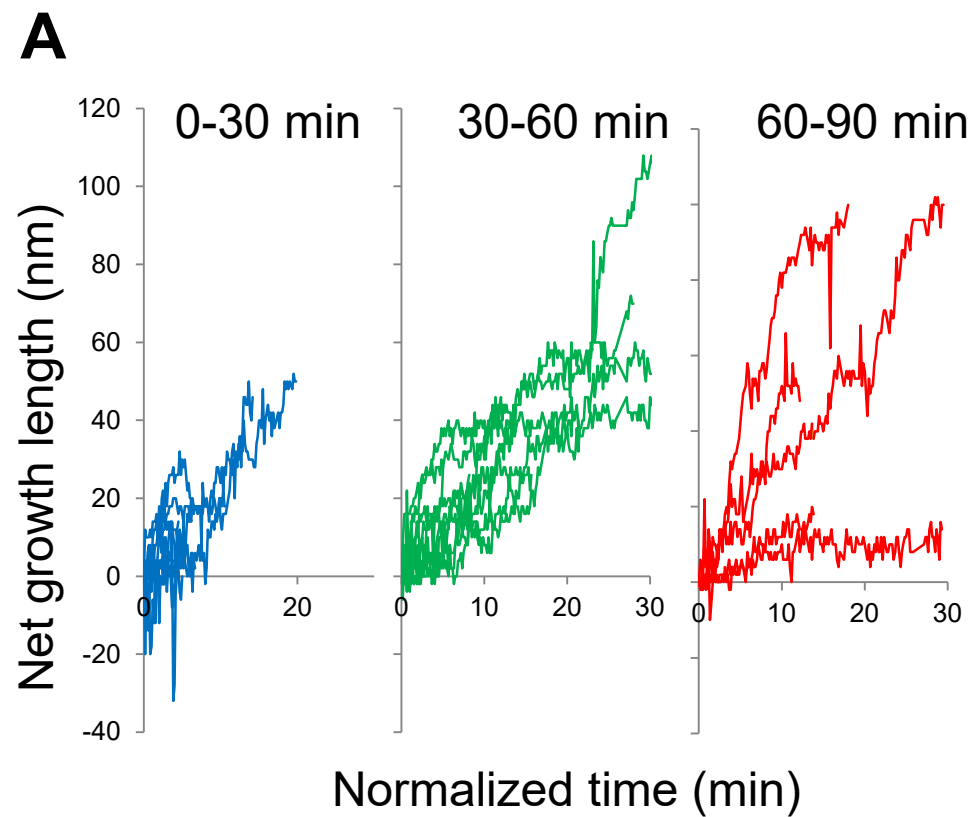


Fig. S4

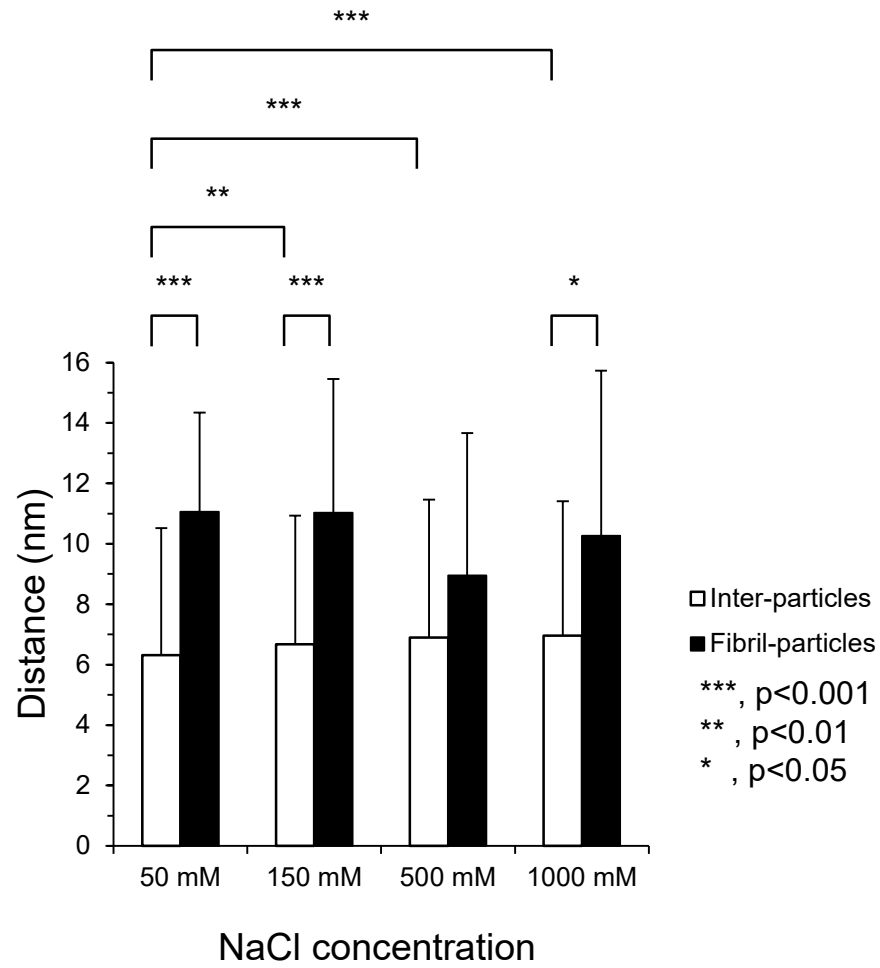
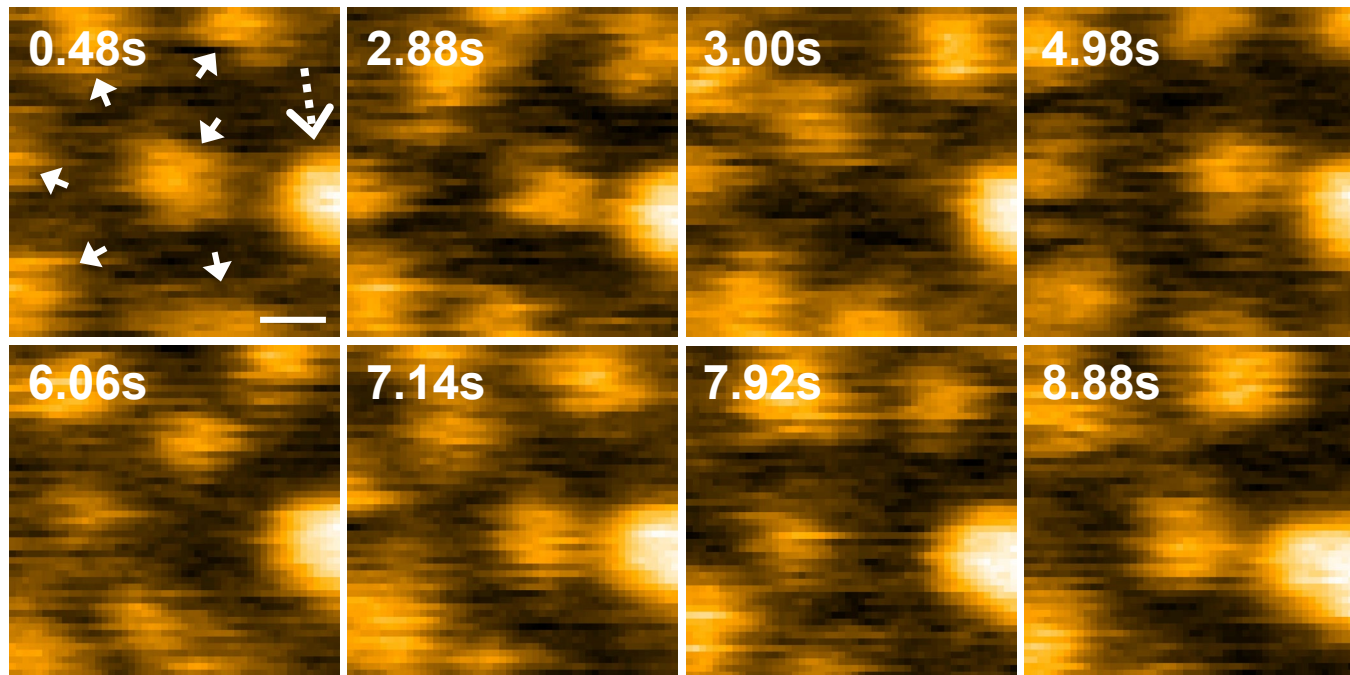


Fig. S5

A



B

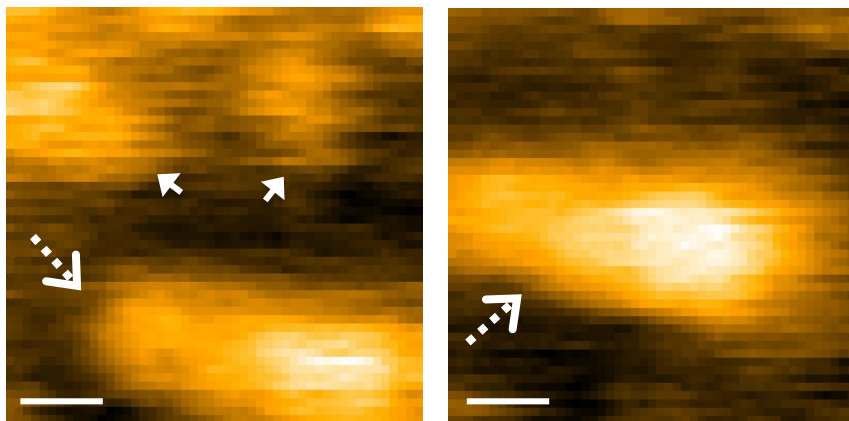


Fig. S6

